

Results of preliminary investigations into multifractal analysis of airborne geophysical data

Lilantha Tennekoon, Michel C. Boufadel, and Jonathan E. Nyquist*, Temple University

Summary:

Geophysical measurements of electrical conductivity, magnetic fields, and gamma radiation at the Oak Ridge Reservation exhibited multifractality (fractal and multiscaling), to varying degrees, in both the north-south and east-west directions. The multiscaling was anisotropic, and the underlying statistics of the fields were in general non-Gaussian. We fitted the multifractal model of Schertzer and Lovejoy to the data. The model appears to be able to simulate a wide range of fields and to reproduce the negative skewness of the data histograms. For brevity, only our analysis of the magnetic data is reported here.

Introduction:

A meaningful statistical characterization of a geophysical field requires evaluation of not only the statistics of the field at a point, but also a model of the spatial structure from the correlation function and the variogram. This work explores fitting fractal statistical models to data of electrical conductivity, gamma radiation, and magnetic fields obtained at the Oak Ridge Reservation. Fractals belong to the category of scaling models that assume that the data values at different scales are related through a transformation that involves only the scale ratio (*i.e.*, there is no characteristic length scale).

Our choice of fractals as a model for soil and rock properties is motivated by previous works in the field. Pilkington and Todoeschuck (1993) analyzed magnetic data using Fourier techniques, and found the spatial power spectrum to decay as $k^{-\beta}$, where k is the wave number and β is a real number such that, $2 \leq \beta \leq 4$. Such a power law behavior evidences a scaling regime. These findings were confirmed by Pilkington and Todoeschuck (1995). Recently, Maus et al. (1999) conducted variogram analysis on magnetic data in Canada and found the data to exhibit scaling behavior as function of the horizontal distance.

We now provide a brief review of existing fractal approaches, emphasizing the necessity for using multifractals, a relatively new category of fractals. Topography (*i.e.*, land surface elevation) is used to illustrate the ideas.

Monofractals vs. Multifractals:

Topography has often been cited as an example of scaling processes in nature; when the topographic surface over a small region is properly magnified, it becomes indistinguishable from the topographic surface over a larger region. This means that there is no characteristic length

scale. It is for this reason that experienced geologists do not show a picture of a landscape without including a well-known object for scale, such as a rock hammer or a person.

If one treats land surface elevation as monofractal and plots a vertical transect as a function of space, one obtains a profile that is a monofractal curve that has the fractal dimension D , where $1 < D \leq 2$. The fractal dimension D (more specifically known as the Hausdorff dimension) is a measure of the space-filling ability of the curve. As D decreases, the field becomes smoother (*i.e.* less space-filling) because it is approaching a smooth curve, whose dimension is 1. In such a case, the trend dominates the local variability. Conversely, when D approaches 2, the curve becomes more irregular (*i.e.*, more space-filling) and the trend disappears in favor of increased variability. In the limit, the curve fills an area, whose dimension is 2.

Fractals are like regular objects, when a fractal set of dimension D intersects a plane, the resulting intersection set has the dimension $D_s = D-1$. When the surface is assumed to be monofractal, D_s takes only one value independent of the threshold value, which is not realistic; one expects the number of points (hence D_s) to decrease with increasing T . The multifractal framework is more realistic because it consists of “constructing” the topographic profile based on an infinite number of intersection sets, each having a fractal dimension $D_s(T)$, such that $0 < D_s(T) \leq 1$, where the dependence on the threshold value is explicitly shown. The topographic surface would thus represent an infinite hierarchy of embedded fractal dimensions, each dependent on the threshold value T .

Scaling properties of a physical quantity such as topography or magnetic field may be characterized using the structure function (Boufadel *et al.*, 2000):

$$\langle |\Delta G_s|^q \rangle = \langle |G(x) - G(x+s)|^q \rangle \approx s^{\xi(q)} \quad (1)$$

where s is the spatial lag, the symbol \approx means proportionality within slowly varying quantities, such as $\log s$, and the brackets imply ensemble averages. $\xi(q)$ is known as the structure function exponent. Eq. 1 generalizes the use of the variogram ($q=2$) to include lower and high order moments.

This generalization is needed in case the process is multifractal. Eq. 1 states that the structure function (*e.g.*, the variogram) is a power law function of the lag. This is a useful property, because it indicates that it suffices to know $\xi(q)$ using one value of the lag to fully characterize the

Multifractal analysis of airborne geophysical data

variability of G at any other lag. To assess if a process is scaling, one computes $\langle |G_s|^q \rangle$ for a certain value of q (say $q=2$) for various values of the lag s , and plots $\log \langle |G_s|^q \rangle$, as a function of $\log s$. If the resulting graph is linear (or may be approximated as linear), then the quantity G is scaling. To discern if the process is simple scaling (*i.e.*, monofractal) or multiscaling (*i.e.*, multifractal), one uses many values of q and computes the slope, $\xi(q)$, of $\log \langle |G_s|^q \rangle$ versus $\log s$. One then plots $\xi(q)$ as a function of q . If $\xi(q)$ varies linearly with q (say up to $q < 4$) then G is monofractal. On the other hand, if $\xi(q)$ is nonlinear convex (downward facing), then G is multifractal.

Loosely put, taking various moment orders is equivalent to looking at the spatial variability of the data using different “filters”, each providing different information. Usually large values of q accentuate the role of the large values in the field, while small q values accentuate the small values. Further comparison between monofractal and multifractal can be found elsewhere (Lovejoy *et al.* 1995; Boufadel *et al.*, 2000; Tennekoon *et al.*, 2003).

The discussion above does not depend on adopting a multifractal model, but such a model simplifies the analysis and allows generations of stochastic realizations. We will use for this purpose the multifractal model developed by Schertzer and Lovejoy (1987). In the S&L model the structure function exponent (Eq. 1) is given by:

$$\xi(q) = qH - \frac{c1}{\alpha - 1} (q^\alpha - q), \quad (2)$$

which models the exponent as a function of the parameters, H , α , and $c1$. H is a parameter that is commonly in the range $[0, 1]$. As α decreases, the frequency of sudden large jumps in the random field increases. The parameter $c1$ is known as the scale parameter. It is equal to half the variance when $\alpha = 2$, and plays a similar role for $\alpha < 2$ (*i.e.*, it is a measure of the width of the distribution). As $c1$ increases, the magnitudes of the sudden large jumps increase (Boufadel *et al.*, 2000). Studies have shown that the S&L model is flexible in fitting observed data (Schmitt *et al.*, 1995; Liu and Molz, 1997; Tennekoon *et al.*, 2003). Hence, knowledge of the values of the parameters α , $c1$, and H is sufficient to characterize a field and to generate stochastic realizations of the field.

Sample Airborne Geophysical Data Set:

The geophysical data analyzed here were obtained from a survey in 1993-1994, at the Oak Ridge Reservation (ORR) in Tennessee (Doll *et al.*, 2000). The survey was conducted by flying a helicopter over a large area of the ORR, and collecting electromagnetic, radiometric, and magnetic measurements using sensors attached to or suspended below the helicopter. For this study, we chose only data from

a small, undeveloped region within the ORR to minimize the effects of human impact on the geophysical measurements. Only the magnetic data (Fig 1.) will be presented here due to space constraints.

The size of the region is about 14,000 feet (4267.2 m) in the grid north-south direction by about 7,000 feet (2133.6 m) in the grid east-west direction. The computations in this study are all conducted along the ORR grid coordinates. The geology in this area is comprised of shales, sandstones and carbonates dipping at approximately 45° and striking grid E-W. The flight paths of the helicopter were along grid N-S and data from a total of 51 flight paths of varying length were available for this region.

Because the data were collected at about an altitude of roughly 100 ft, the footprint of sensors (*i.e.*, portion covered by the sensor) is estimated to be roughly about 100 ft; each measurement is an average value over a 100 ft by 100 ft area. Therefore, regardless of the geology, one would expect adjacent readings along the flight path to show positive correlation for separations less than 100 ft.

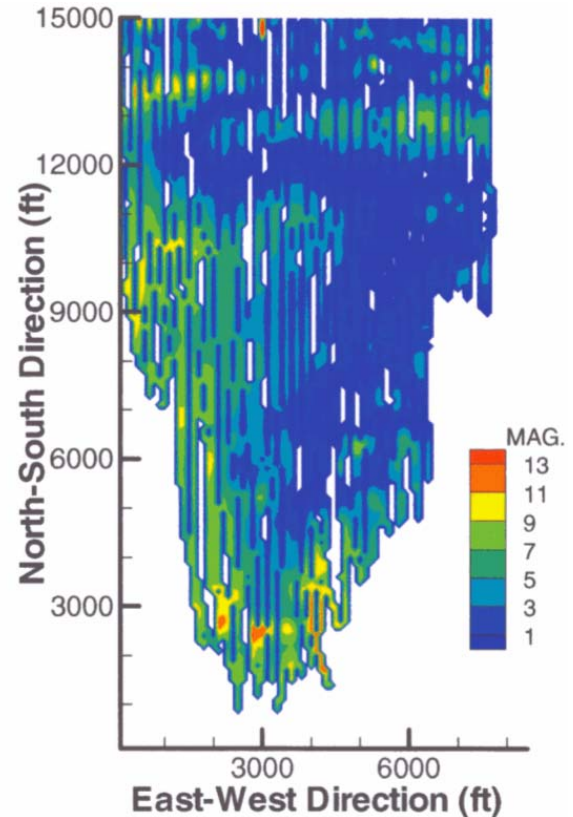


Figure 1: The absolute value of the vertical gradient (nT/m) at the 100 ft grid resolution.

Multifractal analysis of airborne geophysical data

Multifractal Analysis:

spatial average of the replicates. In the north-south direction, there were 75 transects each containing approximately 140 measurement values (total length is about 14,000 ft minus missing points). In the east-west, there were a total 140 transects each containing about 75 measurements (total length in the west-east direction is about 7,500 ft minus missing points). The structure functions were computed for q varying from 0 to 4 at an increment of 0.1 (*i.e.*, a total of 41 orders of moments). The lag distances (s) were selected such that, for each s , there is a minimum of at least 100 measurement pairs from all transects. Such a high number was intended to ensure a sufficient amount of averaging for the SF values.

The analysis of the data was performed along two major directions: north-south and east-west. To facilitate this computation, the data were arranged to fit into straight parallel transects in both directions. This was achieved by dividing the area into a 2D grid, and assigning for each grid point a measurement value, if a measurement was available within the individual grid area. Multiple measurements within a cell were averaged. We were thus able to construct a series of parallel transects, in both directions, with some missing data in between. In each direction, parallel transects were considered as replicates. Square grid sizes of 10 ft, 20 ft, 50 ft, and 100 ft were selected for each of the three data sets. The 100 ft grid size computation performed more averaging of the measurement values, since values that fell within a 100 ft by 100 ft area were averaged and assigned as one value. However, the final results did not vary by any considerable amount amongst the different resolutions. For brevity, we only present the results for the grid size of 100 ft by 100 ft. Choosing a square grid size of 100 ft had the advantage of taking into consideration the footprint of the measurement (roughly about 100 ft a side) and of minimizing the number of missing data points. The disadvantage was the low resolution, since information below 100 ft is not obtainable.

The computed structure functions are plotted for selected values of q on Log-Log plots in Fig. 2. The exponents $\xi(q)$ were then estimated by fitting to the linear part of the plots. It is observed that there is a large spatial range over which scaling is present.

Given that the data exhibit scaling, we now investigate in whether the data are monofractal (monoscaling) or multifractal (multiscaling). As discussed in the theory section, a linear behavior of $\xi(q)$ as a function of q implies monofractality, whereas a nonlinear behavior (namely curvature that results in a downward facing curve) implies multifractality.

The empirical $\xi(q)$ for the magnetic data is plotted in Fig 3. as a function of q . The S&L structure function exponent

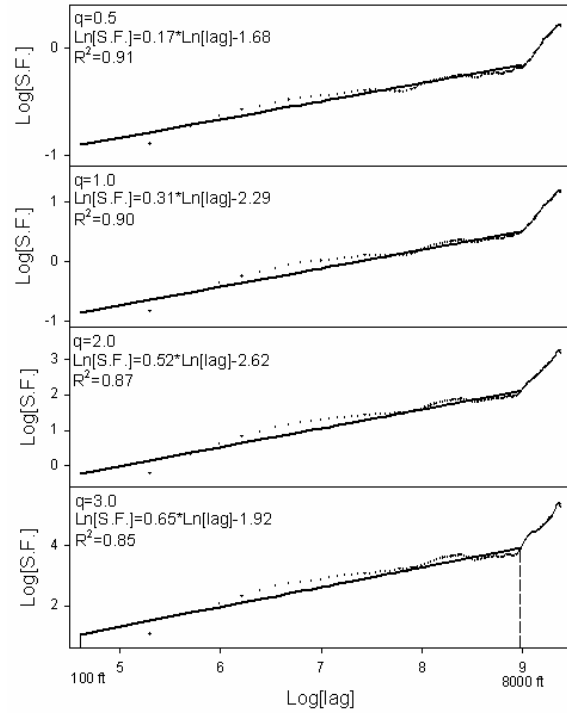


Figure 2: Logarithm of the N-S structure functions for the magnetic data. Scaling is observed from 100 ft to 8000 ft. The E-W results are similar.

(Eq. 2) was fitted to each of these curves (shown as lines in the plots), and the parameters α , $c1$, and H were estimated. Fig 3. shows good evidence of multifractality in the data.

To further evaluate the suitability of the Schertzer & Lovejoy model to simulate the geophysical data, we conducted a probability density function (PDF, or histogram) comparison. We generated ten realizations of a one-dimensional discrete cascade (Boufadel *et al.*, 2000) using the estimated multifractal values (α and $c1$) for each field in both directions. Each realization was the result of ten cascade steps. Hence, they contained $2^9=512$ data points. Each realization was then fractionally integrated to its respective order H value. The PDFs of the logarithm of the generated data are plotted along with the PDFs of the logarithms of the observed data in Fig. 4.

Conclusions:

Prior studies (Pilkington and Todoeschuck, 1993; Pilkington *et al.*, 1994; Pilkington and Todoeschuck, 1995; Maus *et al.*, 1999) found that the spatial distribution of magnetic data exhibit monofractal scaling. Our approach is more general because it allows for multifractality, while treating monofractality as a particular case. It is thus the first appli-

Multifractal analysis of airborne geophysical data

cation of multifractals to airborne geophysical data. Although the theory section contained detailed comparison between monofractals and multifractals, we would like to stress that there is a conceptual leap going from monofractals to multifractals. Monofractals have been traditionally used to describe the shape of geometric objects, such as coastlines, snow flakes. Multifractals have been used to describe the variation of quantities (i.e., fields) over space (or time). One of the well known early applications of multifractals was in the field of turbulence to describe the variation of (turbulent) velocity over space (see the seminal work of Frisch and Parisi, 1985). Multifractal modeling of data allows for simulation of geophysical data across a wide range of scales based on a few simple scaling parameters. Readers interested in further comparison between monofractals and multifractals are urged to read the theory section and references therein.

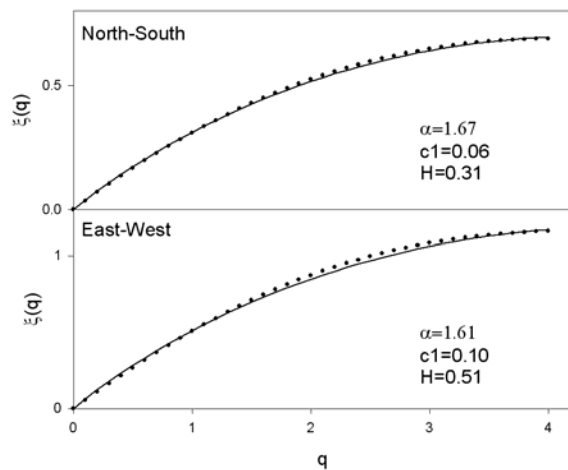


Figure 3: Plot of the observed structure function exponent as a function of the order of moment for the magnetic data. The fit of Eq. 5 (denoted by the line) and the estimated parameters are also shown. The nonlinear, convex shape of the curves implies multifractal behaviour.

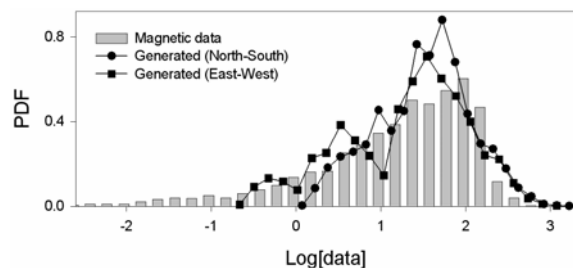


Figure 4: Comparison of the probability density functions (PDFs) between the observed and the generated data. The generated data are able to reproduce the negative skewness of the measured data.

References:

- Boufadel, M. C., S. Lu, F. J. Molz and D. Lavalée, 2000, Multifractal scaling of the intrinsic permeability, *Water Resources Res.*, **36**, 3211-3222.
- Doll, W. E., J. E. Nyquist, L. P. Beard and T. J. Gamey, 2000, Airborne geophysical surveying for hazardous waste site characterization on the Oak Ridge Reservation, Tennessee, *Geophysics*, **65**, 1372-1387.
- Frisch, U. and G. Parisi, 1985, On the singularity structure of fully developed turbulence, *in* *Turbulence and Predictability in Geophysical Fluid Dynamics*, edited by M. Ghil, R. Benzi and G. Parisi, Elsevier, 84-88.
- Liu, H. H. and F. J. Molz, 1997, Multifractal analyses of hydraulic conductivity distributions, *Water Resources Res.*, **33**, 2483-2488.
- Lovejoy, S., D. Lavalée, D. Schertzer and P. Ladoy, 1995, The $1^{1/2}$ law and multifractal topography: Theory and analysis, *Nonlinear Processes Geophys.*, **2**, 16-22.
- Maus, S., K. P. Sengpiel, B. Rottger, B. Siemon and E. A. W. Tordiffe, 1999, Variogram analysis of helicopter magnetic data to identify paleochannels of the Omaruru river, Namibia, *Geophysics*, **64**, 785-794.
- Pilkington, M. and J. P. Todoeschuck, 1993, Fractal magnetization of continental crust, *Geophys. Res. Lett.*, **20**, 627-630.
- Pilkington, M. and J. P. Todoeschuck, 1995, Scaling nature of crustal susceptibilities, *Geophys. Res. Lett.*, **22**, 779-782.
- Schertzer, D. and S. Lovejoy, 1987, Physical modeling and analysis of rain and clouds by anisotropic scaling multiplicative processes, *J. Geophys. Res.*, **92**, 9693-9714.
- Schmitt, F., S. Lovejoy and D. Schertzer, 1995, Multifractal analysis of the Greenland ice-core project climate data, *Geophys. Res. Lett.*, **22**, 1689-1692.
- Tennekoon, L., M. C. Boufadel, D. Lavalée and J. Weaver, 2003, Multifractal anisotropic scaling of the hydraulic conductivity, *Water Resources Res.*, **39**, 1193.